



Article

# General Construction of Amine via Reduction of N=X (X = C, O, H) Bonds Mediated by Supported Nickel Boride Nanoclusters

Da Ke <sup>1,2</sup> and Shaodong Zhou <sup>1,2,\*</sup>

<sup>1</sup> Zhejiang Provincial Key Laboratory of Advanced Chemical Engineering Manufacture Technology, College of Chemical and Biological Engineering, Zhejiang University, Hangzhou 310027, China

<sup>2</sup> Institute of Zhejiang University—Quzhou, Zheda Rd. #99, Quzhou 324000, China

\* Correspondence: szhou@zju.edu.cn

**Abstract:** Amines play an important role in synthesizing drugs, pesticides, dyes, etc. Herein, we report on an efficient catalyst for the general construction of amine mediated by nickel boride nanoclusters supported by a TS-1 molecular sieve. Efficient production of amines was achieved via catalytic hydrogenation of N=X (X = C, O, H) bonds. In addition, the catalyst maintains excellent performance upon recycling. Compared with the previous reports, the high activity, simple preparation and reusability of the Ni-B catalyst in this work make it promising for industrial application in the production of amines.

**Keywords:** nickel boride; primary amine; hydrogenation; reductive amination



**Citation:** Ke, D.; Zhou, S. General Construction of Amine via Reduction of N=X (X = C, O, H) Bonds Mediated by Supported Nickel Boride Nanoclusters. *Int. J. Mol. Sci.* **2022**, *23*, 9337. <https://doi.org/10.3390/ijms23169337>

Academic Editor: Albert Poater

Received: 18 July 2022

Accepted: 16 August 2022

Published: 19 August 2022

**Publisher's Note:** MDPI stays neutral with regard to jurisdictional claims in published maps and institutional affiliations.



**Copyright:** © 2022 by the authors. Licensee MDPI, Basel, Switzerland. This article is an open access article distributed under the terms and conditions of the Creative Commons Attribution (CC BY) license (<https://creativecommons.org/licenses/by/4.0/>).

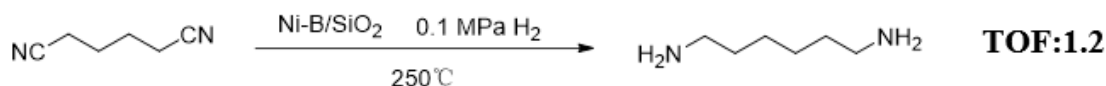
## 1. Introduction

Amine constitutes a vital class of chemicals abundantly existing in nature, and are widely used in industry to produce pharmaceutical drugs, agrochemicals, fine chemicals, polymers, dyes, perfumes, pigments, etc. [1–6]. In recent years, great efforts have been conducted on the synthesis of primary amines. At present, primary amines can be prepared via direct amination of alcohols [7,8], reductive amination of aldehydes or ketone compounds [9–11], amination of carboxylic acids [12,13], and reduction of nitriles [14–18], nitro compounds [19–21], or amides [22]. Among these methods, the reduction of N=X (X = C, O, H) bonds plays a key role. Generally, nitriles, nitro compounds and amides can be reduced to primary amines using borane [21,23,24], silane [25], hydrides [26], formats [20,27], alcohols [28], or molecular hydrogen [29]. Since Raney Ni was first prepared in 1905, it has become one of the most important catalysts for reduction. Though Raney Ni is indeed active, it suffers from high inflammability [30]. To improve this, researchers have developed a variety of homogeneous or heterogeneous catalysts. For example, non-precious metals, such as iron [31–36], cobalt [37–47], copper [48,49], nickel [10,11,21,24,50–53], manganese [6,54,55], and noble metals, such as palladium [19,56–58], platinum [59], ruthenium [8,60–62], rhodium [28,63–65], samarium [66], and iridium [67], have been employed to construct hydrogenation catalysts.

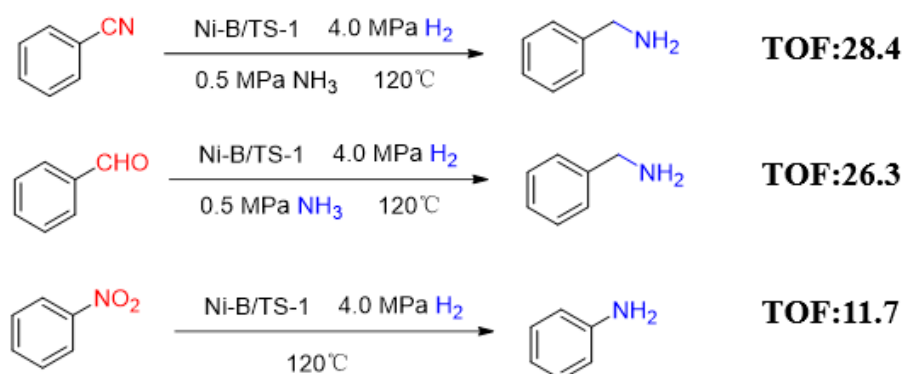
Efficient, stable, and economical hydrogenation catalysts to synthesize primary amines continue to be demanding in both academia and industry. Amorphous nickel boride is well known for its short-range ordered and long-range disordered structures, as well as their activity in liquid phase hydrogenation [68]. Li et al. [69] used Ni-B/SiO<sub>2</sub> as a catalyst to reduce adiponitrile with good selectivity and a low TOF of 1.2 (Scheme 1). At present, there exists only a few reports on the reduction of unsaturated bonds mediated by nickel boride [70,71]. Additionally, the unique pore structure, large specific surface area and excellent hydrothermal stability of titanium silicalite molecular sieves make them widely used in the chemical industry, environmental protection and energy conversion [72–74].

The diffusion path length and the aforementioned characteristics enable titanium silicalite (TS-1) molecular sieves to perform strongly as catalysts. Herein, we report on a nickel boride catalyst with TS-1 as support, for the reduction of N=X (X = C, O, H) bonds to amines with high efficiency and universality (Scheme 1).

Previous work:



This work:



**Scheme 1.** The formation of primary amines.

## 2. Results and Discussion

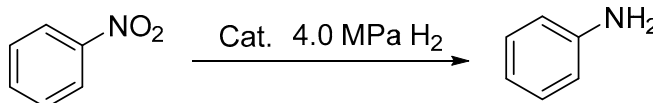
### 2.1. Catalyst Evaluation

We first examined the performances of the catalysts prepared under different conditions, including temperature, pressure, additive and solvent. More details are listed in Table S1. Three reactions were selected to evaluate the catalysts, i.e., the hydrogenation of benzonitrile, nitrobenzene, and the reductive amination of benzaldehyde. The detailed results are shown in Tables 1–3.

**Table 1.** Catalyst screening for benzonitrile <sup>a</sup>.

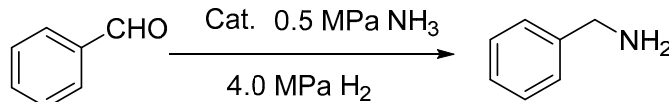
	Catalyst (mg)	Conversion (%) <sup>b</sup>	Yield (%) <sup>c</sup>	TOF (h <sup>-1</sup> ) <sup>d</sup>
1	Ni <sub>6,2</sub> -30 (100)	99	74	23.4
2	Ni <sub>6,2</sub> -50 (100)	100	71	21.9
3	Ni <sub>6,2</sub> -70 (100)	99	66	18.8
4	Ni <sub>6,2</sub> -100 (100)	100	60	17.2
5	Ni <sub>2,5</sub> -30 (250)	100	68	19.0
6	Ni <sub>12,4</sub> -30 (50)	100	77	28.4
7	Ni <sub>18,6</sub> -30 (33)	77	51	22.2
8	Ni <sub>24,8</sub> -30 (25)	71	47	12.7

<sup>a</sup> Reaction condition: 5.0 mmol benzonitrile, 4.0 MPa H<sub>2</sub>, 20 mL of isopropanol, 120 °C. <sup>b</sup> Conversion was calculated by GC. <sup>c</sup> Isolated yield. <sup>d</sup> TOF was the amount of benzonitrile converted by per mol Ni in an hour.

**Table 2.** Reduction of nitrobenzene by different catalysts <sup>a</sup>.


	Catalyst (mg)	Conversion (%) <sup>b</sup>	Yield (%) <sup>c</sup>	TOF (h <sup>-1</sup> ) <sup>d</sup>
1	Ni <sub>6,2</sub> -30 (100)	100	96	5.9
2	Ni <sub>6,2</sub> -50 (100)	100	95	5.6
3	Ni <sub>6,2</sub> -70 (100)	100	95	5.1
4	Ni <sub>6,2</sub> -100 (100)	100	94	4.3
5	Ni <sub>2,5</sub> -30 (250)	85	81	2.9
6	Ni <sub>12,4</sub> -30 (50)	100	97	9.5
7	Ni <sub>18,6</sub> -30 (33)	100	95	11.7
8	Ni <sub>24,8</sub> -30 (25)	100	94	10.5

<sup>a</sup> Reaction condition: 5.0 mmol nitrobenzene, 4.0 MPa H<sub>2</sub>, 20 mL of isopropanol, 120 °C. <sup>b</sup> Conversion was calculated by GC. <sup>c</sup> Isolated yield. <sup>d</sup> TOF was the amount of nitrobenzene converted by per mol Ni in an hour.

**Table 3.** Reduction of aldehyde-ammonia by different catalysts <sup>a</sup>.


	Catalyst (mg)	Conversion (%) <sup>b</sup>	Yield (%) <sup>c</sup>	TOF (h <sup>-1</sup> ) <sup>d</sup>
1	Ni <sub>6,2</sub> -30 (100)	100	92	21.5
2	Ni <sub>6,2</sub> -50 (100)	100	97	19.0
3	Ni <sub>6,2</sub> -70 (100)	100	96	15.8
4	Ni <sub>6,2</sub> -100 (100)	100	95	14.8
5	Ni <sub>2,5</sub> -30 (250)	100	93	19.0
6	Ni <sub>12,4</sub> -30 (50)	100	96	23.7
7	Ni <sub>18,6</sub> -30 (33)	100	96	26.3
8	Ni <sub>24,8</sub> -30 (25)	100	95	22.6

<sup>a</sup> Reaction condition: 5.0 mmol benzaldehyde, 0.5 MPa NH<sub>3</sub> and 4.0 MPa H<sub>2</sub>, 20 mL of isopropanol, 120 °C. <sup>b</sup> Conversion was calculated by GC. <sup>c</sup> Isolated yield. <sup>d</sup> TOF was the amount of benzaldehyde converted by per mol Ni in an hour.

During the reduction of benzonitrile, the imine intermediate would react with primary amine to generate N-benzylidenebenzylamine (B) and further hydrogenated to dibenzylamine (C). Generally, excessive ammonia can inhibit the side reaction with the primary amine [75]. Moreover, acetylation reactions, using highly acidic or basic additives, can also promote the selectivity of primary amines [76–78]. In the model reaction, ammonia was not added to the reaction system in order to evaluate the intrinsic performance of the catalysts. Surprisingly, highly selective generation of primary amines was facilitated. It turned out that both the preparation temperature and the Ni content affect the performance of the catalyst: lower temperature favors a high activity of the catalyst, while a Ni content ~12% is optimal for the catalytic efficiency.

Methanol, ethanol, isopropanol and toluene were tested as the solvent (Figure S1), and isopropanol outperformed the others.

The reaction temperature and hydrogen pressure were simply screened (Figures S2 and S3), and 120 °C and 4.0 MPa were shown to be optimal.

Next, as shown in Table 2, a longer time was required to convert nitrobenzene completely, indicative for a slightly lower activity of the catalyst toward nitro reduction. Though a higher Ni content (18.6%) affords a higher TOF, the yield may not be favored.

Further, reductive amination of benzaldehyde was carried out using the nickel boride catalysts. To promote the selectivity of the target product, the critical point is to avoid further conversion of the product. To this end, it is necessary to use excessive ammonia

to suppress the side reaction. As shown in Table 3, when the same amount of nickel was added, the TOF values did not change much.

Considering both the TOF value and the selectivity of the target product, the Ni<sub>12.4</sub>-30 catalyst was selected for further investigation.

## 2.2. Characterization of Ni<sub>12.4</sub>-30

In order to clarify the actual content of metallic Ni in the catalyst, the accurate mass content of Ni was obtained through the ICP-OES test. The theoretical nickel content in the catalyst was 12.4%, and the experimental data was 12.1%, which was the normal error range (Table S2). Thus, there was no loss of Ni during the preparation process.

The XRD pattern of Ni<sub>12.4</sub>-30, shown in Figure 1, indicates that there was no obvious change on the TS-1 support after loading, implying that the loaded nickel boride component possesses an amorphous structure, in line with previous findings [70]. The rest moiety of the catalyst did not exhibit other diffraction peaks, regardless of the reduction temperature and Ni loading (Figure S4). It is worth noting that nickel boride may react with ethanol at high temperatures to form metallic nickel [79]. The characteristic diffraction peaks for metallic nickel were not found in the used catalyst, therefore, the stability of the nickel boride structure was thus justified, ruling out the possibility that metallic nickel generated in-situ serves as the active species.

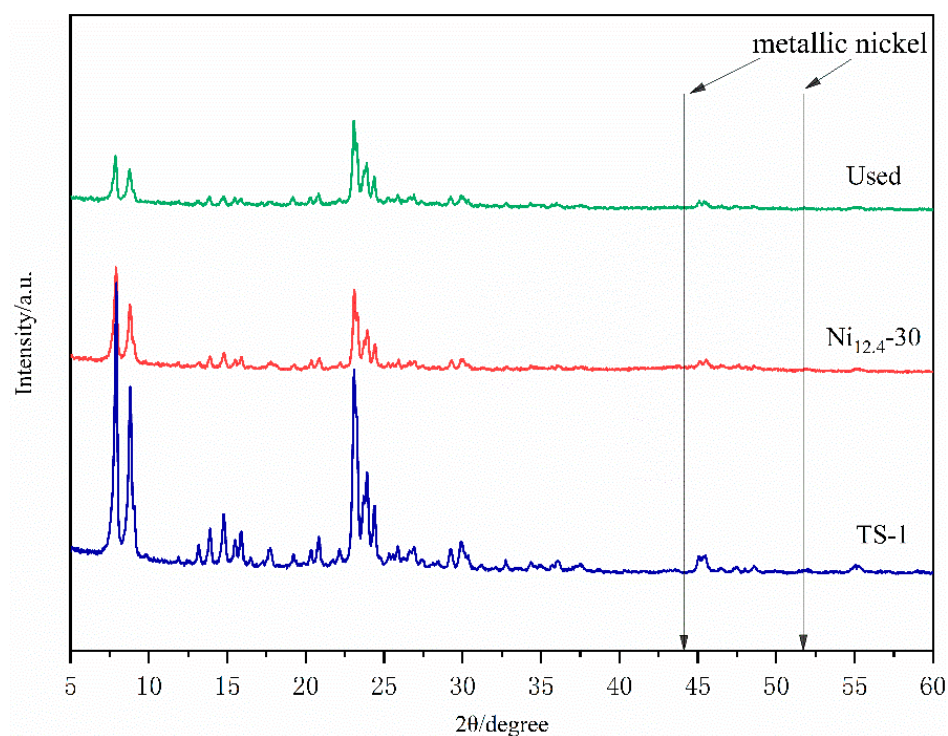


**Figure 1.** XRD pattern of heterogeneous catalyst Ni<sub>12.4</sub>-30.

In order to further identify the chemical state of the catalyst, Ni<sub>12.4</sub>-30 (both the fresh and the recycled ones) were subjected to XPS analysis, and the results are shown in Figure 2. The signals of high-resolution XPS spectra that emerged at around 860 and 190 eV correspond to Ni and B, respectively [80]. The peaks at 853 and 856 eV in Ni 2p<sub>3/2</sub> are ascribed to the metallic nickel and oxidized nickel. The XPS spectrum of pure nickel boride alloy has only one peak of Ni(0), while the peak of Ni(II) appears when nickel boride is supported, in line with previous reports [69–71,81]. The peaks at 188 and 192 eV in B 1s are assigned to elemental and oxidized boron, respectively. The peaks of pure boron in B 1s at 187 eV (< 188 eV) may result from Ni-B interaction. No significant difference in chemical states of Ni and B appears in the used catalyst, indicative of the catalyst's high stability.

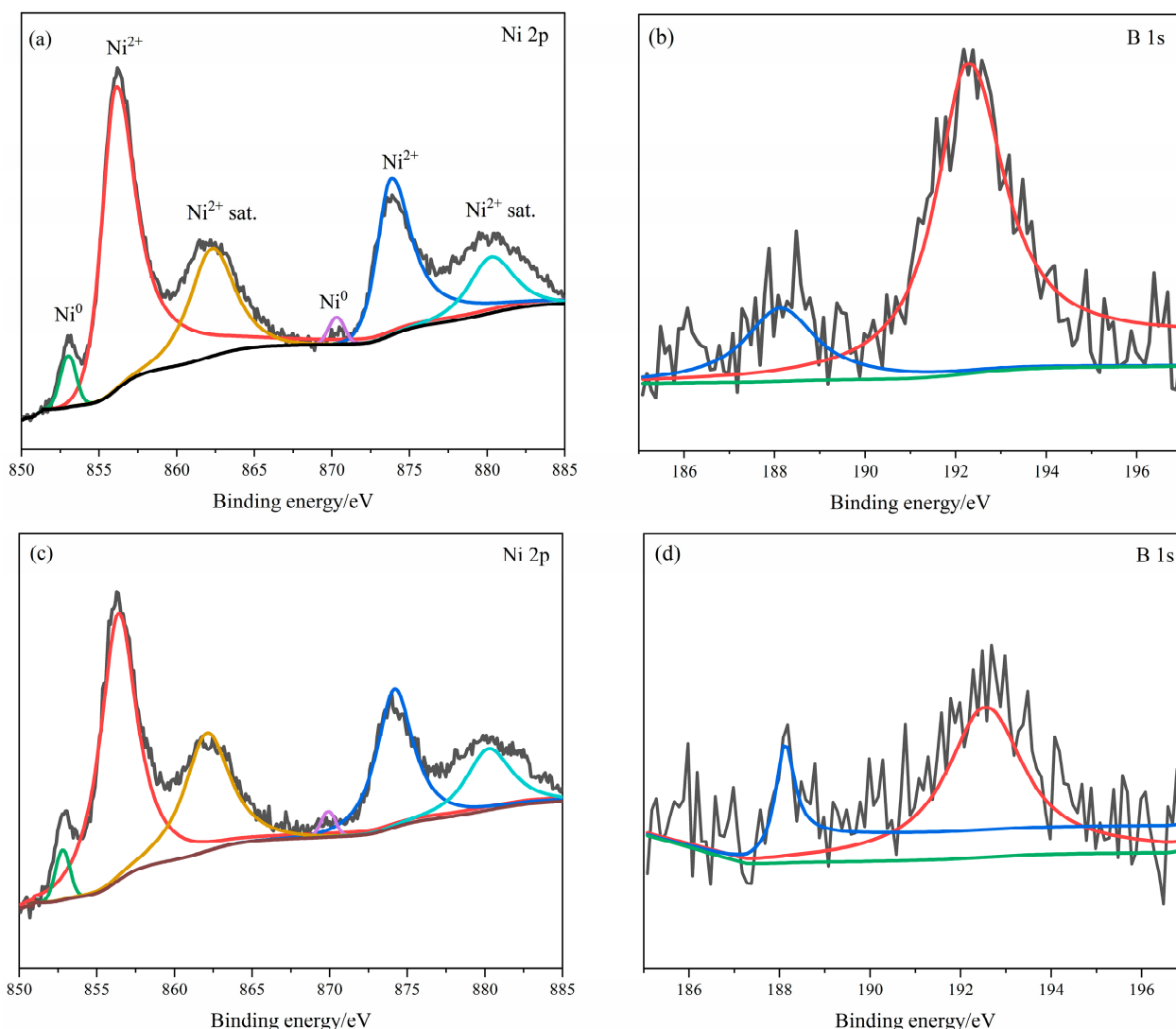


**Figure 2.** (a) Ni 2p, (b) B 1s XPS spectra of fresh catalyst. (c) Ni 2p, (d) B 1s XPS spectra of used catalyst.

The morphologies of the Ni<sub>12.4</sub>-30 catalyst was investigated using TEM. As shown in Figure 3a, the nickel boride species correspond to nanoparticles ranging 10~40 nm diameter with a mean size of 17 nm. A smaller particle size indicates a higher surface energy, and the diameter 17 nm is much smaller than that of pure nickel boride alloy (60 nm) [82], which benefits from the porous structure of TS-1. Most likely, the high activity of this catalyst generates these results. The SAED was employed to determine the crystal structure of nickel boride. There are halo diffraction rings rather than distinct dots in the SAED image, confirming the amorphous structure of nickel boride, in good agreement with XRD patterns. The EDS revealed that the nickel boride comprised of Ni (60%) and B (40%), similar to Ni<sub>2</sub>B.

According to the characteristic results, the high activity of the Ni<sub>12.4</sub>-30 catalyst may result from three aspects. First, the amorphous nickel boride possesses a large number of coordinatively unsaturated active centers on the surface, and a higher surface energy is conducive to the adsorption and conversion of reactants. Second, the electron-transfer from Ni to B causes polarization of the active center and is thus beneficial for Lewis interactions with the reactants. Third, suitable Ni loading dispersed on TS-1 promotes a proper particle size and prevents aggregation, crystallization, and deactivation.

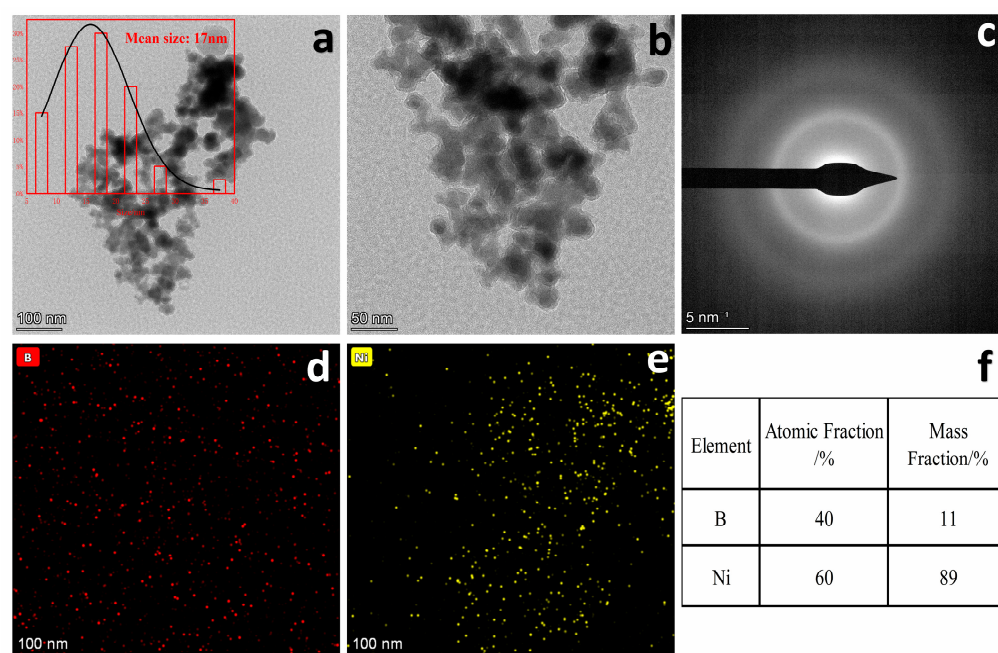


**Figure 3.** TEM images of Ni<sub>12.4</sub>-30 catalyst: (a) 100 nm. (b) 50 nm. (c) SAED pattern. (d) Elemental mapping of B. (e) Elemental mapping of Ni. (f) Elemental composition.

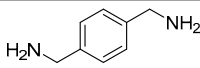
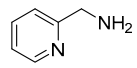
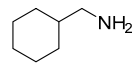
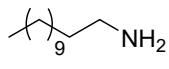
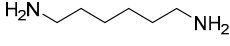
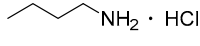
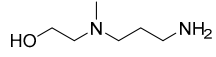
### 2.3. The Reduction of Nitrile

In order to test the universality of the selected catalyst (Ni<sub>12.4</sub>-30), the reduction of various nitriles were carried out under optimal conditions. Ammonia was added into the reaction system to avoid side reactions. Consequently, for most aromatic nitriles, ideal conversion (100%) and primary amines yield (>90%) were obtained (Table 4, entries 1–14). However, when picolinonitrile or 2-aminobenzonitrile were the substrate, a much lower rate of conversion occurred. By contrast, when aliphatic nitriles were subjected to the same conditions, the reaction proceeded very inefficiently (Table 4, entries 15–16, 18–20). It was interesting to note that although the performance of adiponitrile, cyclohexanecarbonitrile and butyronitrile were poor, the performance of dodeconitrile was exceptionally good. This abnormal phenomenon might be ascribed the long carbon chain of dodeconitrile.

**Table 4.** Hydrogenation of nitriles catalyzed by Ni<sub>12.4</sub>-30.

$\text{R-CN} \xrightarrow[\text{0.5 MPa NH}_3]{\text{Cat. 4.0 MPa H}_2} \text{R-CH}_2\text{NH}_2$				
	Product	Time (h)	Conversion (%) <sup>a</sup>	Yield (%) <sup>b</sup>
1	Ph-CH <sub>2</sub> NH <sub>2</sub>	3.5	100	97
2	4-CH <sub>3</sub> -Ph-CH <sub>2</sub> NH <sub>2</sub>	4.0	100	94
3	4-CH <sub>3</sub> O-Ph-CH <sub>2</sub> NH <sub>2</sub>	2.5	100	95
4	4-Cl-Ph-CH <sub>2</sub> NH <sub>2</sub>	3.5	100	95
5	4-NH <sub>2</sub> -Ph-CH <sub>2</sub> NH <sub>2</sub>	4.5	100	97
6	3-CH <sub>3</sub> -Ph-CH <sub>2</sub> NH <sub>2</sub>	4.5	100	96
7	3-CH <sub>3</sub> O-Ph-CH <sub>2</sub> NH <sub>2</sub>	2.5	100	93
8	3-Cl-Ph-CH <sub>2</sub> NH <sub>2</sub>	1.5	100	95
9	3-NH <sub>2</sub> -Ph-CH <sub>2</sub> NH <sub>2</sub>	3.0	100	95
10	2-CH <sub>3</sub> -Ph-CH <sub>2</sub> NH <sub>2</sub>	4.0	100	96
11	2-CH <sub>3</sub> O-Ph-CH <sub>2</sub> NH <sub>2</sub>	4.5	100	92
12	2-Cl-Ph-CH <sub>2</sub> NH <sub>2</sub>	5.0	100	96
13	2-NH <sub>2</sub> -Ph-CH <sub>2</sub> NH <sub>2</sub>	3.0	100	95

Table 4. Cont.

		$\text{R-CN} \xrightarrow[0.5 \text{ MPa NH}_3]{\text{Cat. } 4.0 \text{ MPa H}_2} \text{R-NH}_2$			
	Product	Time (h)	Conversion (%) <sup>a</sup>	Yield (%) <sup>b</sup>	
14		5.0	74.9	69	
15 <sup>c</sup>		8.0	22.1	17	
16 <sup>d</sup>		4.0	63.9	55	
17		8.0	100	97	
18		9.0	68.3	63	
19 <sup>e</sup>		6.0	40.3	35	
20		5.0	<5	-	

Reaction conditions: 5.0 mmol nitrile, 50 mg Ni<sub>12.4</sub>-30 catalyst (about 2.0 mol% Ni), 0.5 MPa NH<sub>3</sub> and 4.0 MPa H<sub>2</sub>, 20 mL of isopropanol, 120 °C. <sup>a</sup> Calculated by GC. <sup>b</sup> Isolated yield. <sup>c</sup> 100 mg catalyst. <sup>d</sup> 110 °C. <sup>e</sup> 20.0 mmol nitrile, 100 mg catalyst, GC yield.

#### 2.4. The Reduction of Nitro Compounds

Further, the catalyst was tested with the hydrogenation of aromatic nitro compounds to primary amines. Under the same conditions to nitrile reduction, more time was needed to convert nitro to amino (see Table 5). In spite of the relatively lower activity toward nitro reduction, the catalyst mediates selective generation of primary amines. The substitution groups on the phenyl ring do not have much effect on the reduction process.

Table 5. Reduction of nitro-aromatic substrates by Ni<sub>12.4</sub>-30.

		$\text{R-NO}_2 \xrightarrow{\text{Cat. } 4.0 \text{ MPa H}_2} \text{R-NH}_2$			
	Product (R)	Time (h)	Conversion (%) <sup>a</sup>	Yield (%) <sup>b</sup>	
1	H	5.0	100	97	
2	4-CH <sub>3</sub>	6.0	100	95	
3	4-F	6.5	100	93	
4	3-F	6.0	100	95	
5	4-Cl	6.5	100	94	
6	4-Br	7.0	100	93	
7 <sup>c</sup>	4-OH	5.5	100	94	
8	4-NH <sub>2</sub>	7.5	100	96	

Reaction conditions: 5.0 mmol nitro compound, 50 mg Ni<sub>12.4</sub>-30 catalyst (about 2.0 mol% Ni), 4.0 MPa H<sub>2</sub>, 20 mL of isopropanol, 120 °C. <sup>a</sup> Calculated by GC. <sup>b</sup> Isolated yield. <sup>c</sup> 1.0 mmol reactant, 10 mg catalyst.

#### 2.5. The Reduction for Aldehyde and Ammonia

Further, the catalytic performance of Ni<sub>12.4</sub>-30 toward reductive amination of aldehyde was examined. Various aldehydes were employed, and the amination results are shown in Table 6. In general, all selected carbonyl compounds were converted to the corresponding amines with excellent yields upon reductive amination. As compared to aromatic aldehydes, aliphatic substrates are relatively less reactive, thus a slightly longer time is required for them to be completely converted.

**Table 6.** Reduction of imines generated by aldehyde and ammonia.

	Product	Time (h)	Conversion (%) <sup>a</sup>	Yield (%) <sup>b</sup>
1	Ph-CH <sub>2</sub> NH <sub>2</sub>	2.0	100	96
2	4-CH <sub>3</sub> -Ph-CH <sub>2</sub> NH <sub>2</sub>	3.0	100	95
3	4-Cl-Ph-CH <sub>2</sub> NH <sub>2</sub>	3.5	100	95
4	4-Br-Ph-CH <sub>2</sub> NH <sub>2</sub>	1.5	100	95
5	4-OH-Ph-CH <sub>2</sub> NH <sub>2</sub>	2.5	100	92
6	3-CH <sub>3</sub> -Ph-CH <sub>2</sub> NH <sub>2</sub>	2.0	100	98
7	3-Cl-Ph-CH <sub>2</sub> NH <sub>2</sub>	3.5	100	92
8	3-Br-Ph-CH <sub>2</sub> NH <sub>2</sub>	2.0	100	96
9	3-OH-Ph-CH <sub>2</sub> NH <sub>2</sub>	1.5	100	92
10	2-CH <sub>3</sub> -Ph-CH <sub>2</sub> NH <sub>2</sub>	2.5	100	98
11	2-Cl-Ph-CH <sub>2</sub> NH <sub>2</sub>	2.0	100	97
12	2-Br-Ph-CH <sub>2</sub> NH <sub>2</sub>	1.0	100	97
13	2-OH-Ph-CH <sub>2</sub> NH <sub>2</sub>	2.0	100	91
14	NH <sub>2</sub> · HCl	4.0	100	>99 <sup>c</sup>

Reaction conditions: 5.0 mmol aldehyde, 50 mg Ni<sub>12.4</sub>-30 catalyst (about 2.0 mol% Ni), 0.5 MPa NH<sub>3</sub> and 4.0 MPa H<sub>2</sub>, 20 mL of isopropanol, 120 °C. <sup>a</sup> Calculated by GC. <sup>b</sup> Isolated yield. <sup>c</sup> GC yield.

In order to test the reusability of the catalyst, the Ni<sub>12.4</sub>-30 species was used fifteen times consecutively with 10 mmol scale. The conversion of benzonitrile, nitrobenzene, and benzaldehyde to amines were all tested. Surprisingly, no obvious loss of activity was observed (Figure 4). Furthermore, the catalytic performance of Ni<sub>12.4</sub>-30 was compared with the commercial Raney Ni (Table 7, see more details in Table S3). For the reduction of benzonitrile, Ni<sub>12.4</sub>-30 catalyst exhibits higher selectivity of benzylamine under ammonia-free conditions. For the other two reactions, there was no obvious difference between Ni<sub>12.4</sub>-30 and Raney Ni.

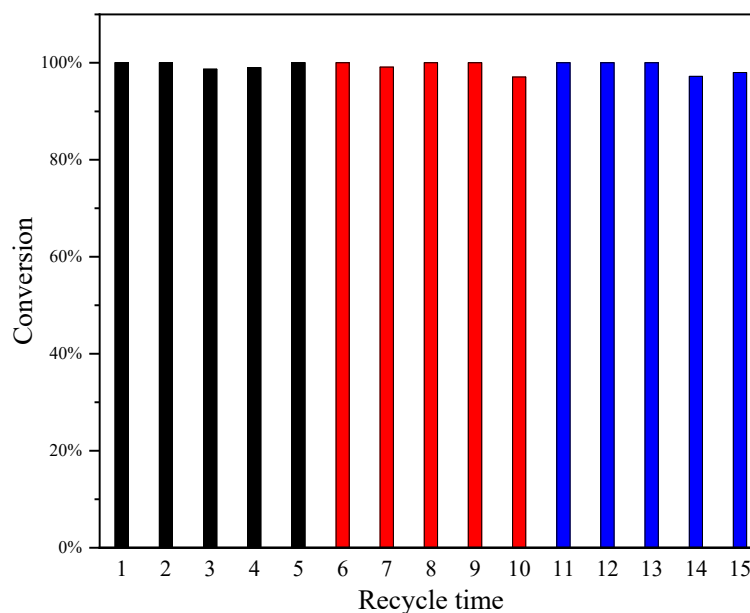


**Figure 4.** Black: benzonitrile. Red: nitrobenzene. Blue: benzaldehyde. The reaction condition: 10 mmol reagent, 100 mg catalyst, 120 °C 4.0 MPa H<sub>2</sub>. When the loss of catalyst reached 20%, the catalyst was replenished, and replenishment was carried out at the 7th and 12th recycles.

**Table 7.** The comparison between two catalysts.

	Catalyst	Time (h)	Conversion (%)	Yield (%)
Benzonitrile	Ni <sub>12.4</sub> -30	3.5	100	77
	Raney Ni	4	100	26
Nitrobenzene	Ni <sub>12.4</sub> -30	5	100	97
	Raney Ni	2	100	97
Benzaldehyde	Ni <sub>12.4</sub> -30	2	100	96
	Raney Ni	3.5	100	92

### 3. Experimental

#### 3.1. Catalyst Preparation

A typical process for catalyst preparation was followed. NiCl<sub>2</sub>·6H<sub>2</sub>O was dissolved in 50 mL deionized water, the TS-1 molecular sieve was added, and this was stirred for 0.5 h at 30 °C. After that, 1 M NaBH<sub>4</sub> solution was added to the suspension while stirring, and stirring continued for 2 h. Finally, the suspension was filtered and washed to obtain a solid catalyst, which was then subjected to vacuum drying at 50 °C for 2 h. The catalyst is named Ni<sub>w</sub>-T, in which “w” and “T” represent the mass content of nickel (compared to TS-1) and the temperature for catalyst preparation, respectively (see more details in the Support Information).

#### 3.2. Catalyst Characterization

ICP data was obtained from Agilent-ICPOES730 (Santa Clara, CA, USA). The X-ray diffraction (XRD) patterns were measured at room temperature using D/max-rA with Cu-K $\alpha$  radiation generated at 10 mA and 40 kV. The X-ray photoelectron spectroscopy (XPS) analysis was carried out by using Thermo Scientific K-Alpha (Waltham, MA, USA) with Al-K $\alpha$  radiation. The morphological information was measured by a transmission electron microscope (TEM) conducted using a Thermo Scientific Talos F200S coupled with X-ray spectroscopy (EDS).

#### 3.3. Catalyst Activity Measurement

Nitrile, catalyst and solvent were mixed in a 100 mL volume autoclave equipped with PTFE and magnetic pellet. The kettle was filled with 0.5 MPa ammonia gas and heated to 120 °C; at this temperature, 4.0 MPa H<sub>2</sub> was pressed in, and then reaction was started. During the process, the system pressure was controlled between 4.0  $\pm$  0.1 MPa. After reaction (under constant pressure), the autoclave was cooled and degassed, the reaction solution was filtered to recover the catalyst, and the filtrate was concentrated to determine the conversion by GC. <sup>1</sup>H NMR and <sup>13</sup>C NMR spectrum data were recorded by a Bruker DRX-400 spectrometer (Billerica, MA, USA) using CDCl<sub>3</sub> or DMSO-d<sub>6</sub> as solvent at 298 K. Gas chromatography (GC) was performed on Agilent chromatography with a SE54 column. More details in support information (for spectra, see Figures S4–S72).

### 4. Conclusions

In conclusion, we have presented a nanostructured nickel boride catalyst that can be used for the efficient reduction of nitrile, nitro compounds, and imine groups. This catalyst was prepared via chemical reduction at room temperature with an average particle size of 17 nm and homogeneous distribution. XRD and SAED justified the amorphous structure of nickel boride. The Ni<sub>12.4</sub>-30 catalyst has been proven to be highly active towards all three reactions, with high TOF values. Furthermore, recycling tests proved that the catalysts are robust for consecutive use. In addition, the performance of the Ni<sub>12.4</sub>-30 catalyst is comparable to commercial Raney Ni, but it is safer for storage. The promising prospect of the nickel boride catalyst for industrial application has thus been proven.

**Supplementary Materials:** The following supporting information can be downloaded at: <https://www.mdpi.com/article/10.3390/ijms23169337/s1>.

**Author Contributions:** Conceptualization, D.K. and S.Z.; methodology, D.K. and S.Z.; writing—original draft preparation, D.K.; writing—review and editing, S.Z. All authors have read and agreed to the published version of the manuscript.

**Funding:** Generous financial support by the National Natural Science Foundation of China (21878265).

**Institutional Review Board Statement:** Not applicable.

**Informed Consent Statement:** Not applicable.

**Data Availability Statement:** Additional figures are available in the Supplementary Materials.

**Conflicts of Interest:** The authors declare no conflict of interest.

## References

1. Ezelarab, H.A.A.; Abbas, S.H.; Hassan, H.A.; Abu-Rahma, G.E.A. Recent updates of fluoroquinolones as antibacterial agents. *Arch. Pharm.* **2018**, *351*, e1800141. [[CrossRef](#)] [[PubMed](#)]
2. Ahmadi, T.; Mohammadi Ziarani, G.; Bahar, S.; Badiie, A. Domino synthesis of quinoxaline derivatives using SBA-Pr-NH<sub>2</sub> as a nanoreactor and their spectrophotometric complexation studies with some metals ions. *J. Iran. Chem. Soc.* **2018**, *15*, 1153–1161. [[CrossRef](#)]
3. Vo, N.B.; Nguyen, L.A.; Pham, T.L.; Doan, D.T.; Nguyen, T.B.; Ngo, Q.A. Straightforward access to new vinca-alkaloids via selective reduction of a nitrile containing anhydrovinblastine derivative. *Tetrahedron Lett.* **2017**, *58*, 2503–2506. [[CrossRef](#)]
4. Wang, P.; Zhao, X.H.; Wang, Z.Y.; Meng, M.; Li, X.; Ning, Q. Generation 4 polyamidoamine dendrimers is a novel candidate of nano-carrier for gene delivery agents in breast cancer treatment. *Cancer Lett.* **2010**, *298*, 34–49. [[CrossRef](#)]
5. Yemul, O.; Imae, T. Synthesis and characterization of poly(ethyleneimine) dendrimers. *Colloid Polym. Sci.* **2008**, *286*, 747–752. [[CrossRef](#)]
6. Garduño, J.A.; García, J.J. Non-Pincer Mn(I) Organometallics for the Selective Catalytic Hydrogenation of Nitriles to Primary Amines. *ACS Catal.* **2018**, *9*, 392–401. [[CrossRef](#)]
7. Mastalir, M.; Stöger, B.; Pittenauer, E.; Puchberger, M.; Allmaier, G.; Kirchner, K. Air Stable Iron(II) PNP Pincer Complexes as Efficient Catalysts for the Selective Alkylation of Amines with Alcohols. *Adv. Synth. Catal.* **2016**, *358*, 3824–3831. [[CrossRef](#)]
8. Baumann, W.; Spannenberg, A.; Pfeffer, J.; Haas, T.; Kockritz, A.; Martin, A.; Deutsch, J. Utilization of common ligands for the ruthenium-catalyzed amination of alcohols. *Chem. Eur. J.* **2013**, *19*, 17702–17706. [[CrossRef](#)]
9. Zhuang, X.; Liu, J.; Zhong, S.; Ma, L. Selective catalysis for the reductive amination of furfural toward furfurylamine by graphene-co-shelled cobalt nanoparticles. *Green Chem.* **2022**, *24*, 271–284. [[CrossRef](#)]
10. Zhang, Y.; Yang, H.; Chi, Q.; Zhang, Z. Nitrogen-Doped Carbon-Supported Nickel Nanoparticles: A Robust Catalyst to Bridge the Hydrogenation of Nitriles and the Reductive Amination of Carbonyl Compounds for the Synthesis of Primary Amines. *ChemSusChem* **2019**, *12*, 1246–1255. [[CrossRef](#)]
11. Hahn, G.; Kunas, P.; de Jonge, N.; Kempe, R. General synthesis of primary amines via reductive amination employing a reusable nickel catalyst. *Nat. Catal.* **2018**, *2*, 71–77. [[CrossRef](#)]
12. Coeck, R.; De Vos, D.E. One-pot reductive amination of carboxylic acids: A sustainable method for primary amine synthesis. *Green Chem.* **2020**, *22*, 5105–5114. [[CrossRef](#)]
13. Citoler, J.; Derrington, S.R.; Galman, J.L.; Bevinakatti, H.; Turner, N.J. A biocatalytic cascade for the conversion of fatty acids to fatty amines. *Green Chem.* **2019**, *21*, 4932–4935. [[CrossRef](#)]
14. Antil, N.; Kumar, A.; Akhtar, N.; Newar, R.; Begum, W.; Dwivedi, A.; Manna, K. Aluminum Metal–Organic Framework-Ligated Single-Site Nickel(II)-Hydride for Heterogeneous Chemoselective Catalysis. *ACS Catal.* **2021**, *11*, 3943–3957. [[CrossRef](#)]
15. Wang, C.; Jia, Z.; Zhen, B.; Han, M. Supported Ni Catalyst for Liquid Phase Hydrogenation of Adiponitrile to 6-Aminocapronitrile and Hexamethylenediamine. *Molecules* **2018**, *23*, 92. [[CrossRef](#)] [[PubMed](#)]
16. Konnerth, H.; Precht, M.H.G. Nitrile hydrogenation using nickel nanocatalysts in ionic liquids. *New J. Chem.* **2017**, *41*, 9594–9597. [[CrossRef](#)]
17. Cheng, H.; Meng, X.; Wu, C.; Shan, X.; Yu, Y.; Zhao, F. Selective hydrogenation of benzonitrile in multiphase reaction systems including compressed carbon dioxide over Ni/Al<sub>2</sub>O<sub>3</sub> catalyst. *J. Mol. Catal. A Chem.* **2013**, *379*, 72–79. [[CrossRef](#)]
18. Segobia, D.J.; Trasarti, A.F.; Apesteguía, C.R. Hydrogenation of nitriles to primary amines on metal-supported catalysts: Highly selective conversion of butyronitrile to n-butylamine. *Appl. Catal. A Gen.* **2012**, *445–446*, 69–75. [[CrossRef](#)]
19. Liu, Y.; He, S.; Quan, Z.; Cai, H.; Zhao, Y.; Wang, B. Mild palladium-catalysed highly efficient hydrogenation of C–N, C–NO<sub>2</sub>, and C–O bonds using H<sub>2</sub> of 1 atm in H<sub>2</sub>O. *Green Chem.* **2019**, *21*, 830–838. [[CrossRef](#)]
20. Martina, K.; Baricco, F.; Tagliapietra, S.; Moran, M.J.; Cravotto, G.; Cintas, P. Highly efficient nitrobenzene and alkyl/aryl azide reduction in stainless steel jars without catalyst addition. *New J. Chem.* **2018**, *42*, 18881–18888. [[CrossRef](#)]
21. Göksu, H.; Ho, S.F.; Metin, Ö.; Korkmaz, K.; Mendoza Garcia, A.; Gültekin, M.S.; Sun, S. Tandem Dehydrogenation of Ammonia Borane and Hydrogenation of Nitro/Nitrile Compounds Catalyzed by Graphene-Supported NiPd Alloy Nanoparticles. *ACS Catal.* **2014**, *4*, 1777–1782. [[CrossRef](#)]

22. Zhang, T.; Zhang, Y.; Zhang, W.; Luo, M. A Convenient and General Reduction of Amides to Amines with Low-Valent Titanium. *Adv. Synth. Catal.* **2013**, *355*, 2775–2780. [[CrossRef](#)]
23. Amberchan, G.; Snelling, R.A.; Moya, E.; Landi, M.; Lutz, K.; Gatihi, R.; Singaram, B. Reaction of Diisobutylaluminum Borohydride, a Binary Hydride, with Selected Organic Compounds Containing Representative Functional Groups. *J. Org. Chem.* **2021**, *86*, 6207–6227. [[CrossRef](#)] [[PubMed](#)]
24. Zen, Y.-F.; Fu, Z.-C.; Liang, F.; Xu, Y.; Yang, D.-D.; Yang, Z.; Gan, X.; Lin, Z.-S.; Chen, Y.; Fu, W.-F. Robust Hydrogenation of Nitrile and Nitro Groups to Primary Amines Using Ni<sub>2</sub>P as a Catalyst and Ammonia Borane under Ambient Conditions. *Asian J. Org. Chem.* **2017**, *6*, 1589–1593. [[CrossRef](#)]
25. Maddani, M.R.; Moorthy, S.K.; Prabhu, K.R. Chemoselective reduction of azides catalyzed by molybdenum xanthate by using phenylsilane as the hydride source. *Tetrahedron* **2010**, *66*, 329–333. [[CrossRef](#)]
26. Zeynizadeh, B.; Mousavi, H.; Mohammad Aminzadeh, F. A hassle-free and cost-effective transfer hydrogenation strategy for the chemoselective reduction of aryl nitriles to primary amines through in situ-generated nickel(II) dihydride intermediate in water. *J. Mol. Struct.* **2022**, 1255. [[CrossRef](#)]
27. Liu, L.; Li, J.; Ai, Y.; Liu, Y.; Xiong, J.; Wang, H.; Qiao, Y.; Liu, W.; Tan, S.; Feng, S.; et al. A ppm level Rh-based composite as an ecofriendly catalyst for transfer hydrogenation of nitriles: Triple guarantee of selectivity for primary amines. *Green Chem.* **2019**, *21*, 1390–1395. [[CrossRef](#)]
28. Podyacheva, E.; Afanasyev, O.I.; Vasilyev, D.V.; Chusov, D. Borrowing Hydrogen Amination Reactions: A Complex Analysis of Trends and Correlations of the Various Reaction Parameters. *ACS Catal.* **2022**, *12*, 7142–7198. [[CrossRef](#)]
29. Lévay, K.; Hegedűs, L. Recent Achievements in the Hydrogenation of Nitriles Catalyzed by Transitional Metals. *Curr. Org. Chem.* **2019**, *23*, 1881–1900. [[CrossRef](#)]
30. Debellefon, C.; Fouilloux, P. Homogeneous and heterogeneous hydrogenation of nitriles in a liquid-phase—Chemical, mechanistic, and catalytic aspects. *Catal. Rev.* **1994**, *36*, 459–506. [[CrossRef](#)]
31. Chandrashekar, V.G.; Senthamarai, T.; Kadam, R.G.; Malina, O.; Kašlík, J.; Zbořil, R.; Gawande, M.B.; Jagadeesh, R.V.; Beller, M. Silica-supported Fe/Fe–O nanoparticles for the catalytic hydrogenation of nitriles to amines in the presence of aluminium additives. *Nat. Catal.* **2021**, *5*, 20–29. [[CrossRef](#)]
32. Chakraborty, S.; Milstein, D. Selective Hydrogenation of Nitriles to Secondary Imines Catalyzed by an Iron Pincer Complex. *ACS Catal.* **2017**, *7*, 3968–3972. [[CrossRef](#)]
33. Lange, S.; Elangovan, S.; Cordes, C.; Spannenberg, A.; Jiao, H.; Junge, H.; Bachmann, S.; Scalone, M.; Topf, C.; Junge, K.; et al. Selective catalytic hydrogenation of nitriles to primary amines using iron pincer complexes. *Catal. Sci. Technol.* **2016**, *6*, 4768–4772. [[CrossRef](#)]
34. Chakraborty, S.; Leitus, G.; Milstein, D. Selective hydrogenation of nitriles to primary amines catalyzed by a novel iron complex. *Chem. Commun.* **2016**, *52*, 1812–1815. [[CrossRef](#)]
35. Mérel, D.S.; Do, M.L.T.; Gaillard, S.; Dupau, P.; Renaud, J.-L. Iron-catalyzed reduction of carboxylic and carbonic acid derivatives. *Coord. Chem. Rev.* **2015**, *288*, 50–68. [[CrossRef](#)]
36. Bornschein, C.; Werkmeister, S.; Wendt, B.; Jiao, H.; Alberico, E.; Baumann, W.; Junge, H.; Junge, K.; Beller, M. Mild and selective hydrogenation of aromatic and aliphatic (di)nitriles with a well-defined iron pincer complex. *Nat. Commun.* **2014**, *5*, 4111. [[CrossRef](#)] [[PubMed](#)]
37. Sheng, M.; Yamaguchi, S.; Nakata, A.; Yamazoe, S.; Nakajima, K.; Yamasaki, J.; Mizugaki, T.; Mitsudome, T. Hydrotalcite-Supported Cobalt Phosphide Nanorods as a Highly Active and Reusable Heterogeneous Catalyst for Ammonia-Free Selective Hydrogenation of Nitriles to Primary Amines. *ACS Sustain. Chem. Eng.* **2021**, *9*, 11238–11246. [[CrossRef](#)]
38. Mitsudome, T.; Sheng, M.; Nakata, A.; Yamasaki, J.; Mizugaki, T.; Jitsukawa, K. A cobalt phosphide catalyst for the hydrogenation of nitriles. *Chem. Sci.* **2020**, *11*, 6682–6689. [[CrossRef](#)]
39. Formenti, D.; Mocci, R.; Atia, H.; Dastgir, S.; Anwar, M.; Bachmann, S.; Scalone, M.; Junge, K.; Beller, M. A State-of-the-Art Heterogeneous Catalyst for Efficient and General Nitrile Hydrogenation. *Chem. Eur. J.* **2020**, *26*, 15589–15595. [[CrossRef](#)]
40. Murugesan, K.; Senthamarai, T.; Sohail, M.; Alshammari, A.S.; Pohl, M.M.; Beller, M.; Jagadeesh, R.V. Cobalt-based nanoparticles prepared from MOF-carbon templates as efficient hydrogenation catalysts. *Chem. Sci.* **2018**, *9*, 8553–8560. [[CrossRef](#)]
41. Ferraccioli, R.; Borovika, D.; Surkus, A.-E.; Kreyenschulte, C.; Topf, C.; Beller, M. Synthesis of cobalt nanoparticles by pyrolysis of vitamin B12: A non-noble-metal catalyst for efficient hydrogenation of nitriles. *Catal. Sci. Technol.* **2018**, *8*, 499–507. [[CrossRef](#)]
42. Dai, H.; Guan, H. Switching the Selectivity of Cobalt-Catalyzed Hydrogenation of Nitriles. *ACS Catal.* **2018**, *8*, 9125–9130. [[CrossRef](#)]
43. Tokmic, K.; Jackson, B.J.; Salazar, A.; Woods, T.J.; Fout, A.R. Cobalt-Catalyzed and Lewis Acid-Assisted Nitrile Hydrogenation to Primary Amines: A Combined Effort. *J. Am. Chem. Soc.* **2017**, *139*, 13554–13561. [[CrossRef](#)] [[PubMed](#)]
44. Adam, R.; Bheeter, C.B.; Cabrero-Antonino, J.R.; Junge, K.; Jackstell, R.; Beller, M. Selective Hydrogenation of Nitriles to Primary Amines by using a Cobalt Phosphine Catalyst. *ChemSusChem* **2017**, *10*, 842–846. [[CrossRef](#)] [[PubMed](#)]
45. Shao, Z.; Fu, S.; Wei, M.; Zhou, S.; Liu, Q. Mild and Selective Cobalt-Catalyzed Chemodivergent Transfer Hydrogenation of Nitriles. *Angew. Chem. Int. Ed.* **2016**, *55*, 14653–14657. [[CrossRef](#)] [[PubMed](#)]
46. Chen, F.; Topf, C.; Radnik, J.; Kreyenschulte, C.; Lund, H.; Schneider, M.; Surkus, A.E.; He, L.; Junge, K.; Beller, M. Stable and Inert Cobalt Catalysts for Highly Selective and Practical Hydrogenation of C≡N and C=O Bonds. *J. Am. Chem. Soc.* **2016**, *138*, 8781–8788. [[CrossRef](#)]

47. Mukherjee, A.; Srimani, D.; Chakraborty, S.; Ben-David, Y.; Milstein, D. Selective Hydrogenation of Nitriles to Primary Amines Catalyzed by a Cobalt Pincer Complex. *J. Am. Chem. Soc.* **2015**, *137*, 8888–8891. [[CrossRef](#)]
48. Segobia, D.J.; Trasarti, A.F.; Apesteguía, C.R. Chemoselective hydrogenation of unsaturated nitriles to unsaturated primary amines: Conversion of cinnamionitrile on metal-supported catalysts. *Appl. Catal. A-Gen.* **2015**, *494*, 41–47. [[CrossRef](#)]
49. van der Waals, D.; Pettman, A.; Williams, J.M.J. Copper-catalysed reductive amination of nitriles and organic-group reductions using dimethylamine borane. *RSC Adv.* **2014**, *4*, 51845–51849. [[CrossRef](#)]
50. Lv, Y.; Hao, F.; Liu, P.; Xiong, S.; Luo, H. Liquid phase hydrogenation of adiponitrile over acid-activated sepiolite supported K–La–Ni trimetallic catalysts. *React. Kinet. Mech. Cat.* **2016**, *119*, 555–568. [[CrossRef](#)]
51. Konnerth, H.; Prechtel, M.H. Selective partial hydrogenation of alkynes to (Z)-alkenes with ionic liquid-doped nickel nanocatalysts at near ambient conditions. *Chem. Commun.* **2016**, *52*, 9129–9132. [[CrossRef](#)] [[PubMed](#)]
52. Jia, Z.; Zhen, B.; Han, M.; Wang, C. Liquid phase hydrogenation of adiponitrile over directly reduced Ni/SiO<sub>2</sub> catalyst. *Catal. Commun.* **2016**, *73*, 80–83. [[CrossRef](#)]
53. Cao, Y.; Niu, L.; Wen, X.; Feng, W.; Huo, L.; Bai, G. Novel layered double hydroxide/oxide-coated nickel-based core-shell nanocomposites for benzonitrile selective hydrogenation: An interesting water switch. *J. Catal.* **2016**, *339*, 9–13. [[CrossRef](#)]
54. Weber, S.; Stoger, B.; Kirchner, K. Hydrogenation of Nitriles and Ketones Catalyzed by an Air-Stable Bisphosphine Mn(I) Complex. *Org. Lett.* **2018**, *20*, 7212–7215. [[CrossRef](#)] [[PubMed](#)]
55. Elangovan, S.; Topf, C.; Fischer, S.; Jiao, H.; Spannenberg, A.; Baumann, W.; Ludwig, R.; Junge, K.; Beller, M. Selective Catalytic Hydrogenations of Nitriles, Ketones, and Aldehydes by Well-Defined Manganese Pincer Complexes. *J. Am. Chem. Soc.* **2016**, *138*, 8809–8814. [[CrossRef](#)]
56. Ma, K.; Liao, W.; Shi, W.; Xu, F.; Zhou, Y.; Tang, C.; Lu, J.; Shen, W.; Zhang, Z. Ceria-supported Pd catalysts with different size regimes ranging from single atoms to nanoparticles for the oxidation of CO. *J. Catal.* **2022**, *407*, 104–114. [[CrossRef](#)]
57. Yoshimura, M.; Komatsu, A.; Niimura, M.; Takagi, Y.; Takahashi, T.; Ueda, S.; Ichikawa, T.; Kobayashi, Y.; Okami, H.; Hattori, T.; et al. Selective Synthesis of Primary Amines from Nitriles under Hydrogenation Conditions. *Adv. Synth. Catal.* **2018**, *360*, 1726–1732. [[CrossRef](#)]
58. Saito, Y.; Ishitani, H.; Ueno, M.; Kobayashi, S. Selective Hydrogenation of Nitriles to Primary Amines Catalyzed by a Polysilane/SiO<sub>2</sub>-Supported Palladium Catalyst under Continuous-Flow Conditions. *ChemistryOpen* **2017**, *6*, 211–215. [[CrossRef](#)]
59. Lu, S.; Wang, J.; Cao, X.; Li, X.; Gu, H. Selective synthesis of secondary amines from nitriles using Pt nanowires as a catalyst. *Chem. Commun.* **2014**, *50*, 3512–3515. [[CrossRef](#)]
60. Muratsugu, S.; Kityakarn, S.; Wang, F.; Ishiguro, N.; Kamachi, T.; Yoshizawa, K.; Sekizawa, O.; Uruga, T.; Tada, M. Formation and nitrile hydrogenation performance of Ru nanoparticles on a K-doped Al<sub>2</sub>O<sub>3</sub> surface. *Phys. Chem. Chem. Phys.* **2015**, *17*, 24791–24802. [[CrossRef](#)] [[PubMed](#)]
61. Segobia, D.J.; Trasarti, A.F.; Apesteguía, C.R. Conversion of butyronitrile to butylamines on noble metals: Effect of the solvent on catalyst activity and selectivity. *Catal. Sci. Technol.* **2014**, *4*, 4075–4083. [[CrossRef](#)]
62. Xie, X.F.; Liotta, C.L.; Eckert, C.A. CO<sub>2</sub>-protected amine formation from nitrile and imine hydrogenation in gas-expanded liquids. *Ind. Eng. Chem. Res.* **2004**, *43*, 7907–7911. [[CrossRef](#)]
63. Rajesh, K.; Dudle, B.; Blacque, O.; Berke, H. Homogeneous Hydrogenations of Nitriles Catalyzed by Rhenium Complexes. *Adv. Synth. Catal.* **2011**, *353*, 1479–1484. [[CrossRef](#)]
64. Chatterjee, M.; Sato, M.; Kawanami, H.; Yokoyama, T.; Suzuki, T.; Ishizaka, T. An Efficient Hydrogenation of Dinitrile to Aminonitrile in Supercritical Carbon Dioxide. *Adv. Synth. Catal.* **2010**, *352*, 2394–2398. [[CrossRef](#)]
65. Monguchi, Y.; Mizuno, M.; Ichikawa, T.; Fujita, Y.; Murakami, E.; Hattori, T.; Maegawa, T.; Sawama, Y.; Sajiki, H. Catalyst-Dependent Selective Hydrogenation of Nitriles: Selective Synthesis of Tertiary and Secondary Amines. *J. Org. Chem.* **2017**, *82*, 10939–10944. [[CrossRef](#)] [[PubMed](#)]
66. Szostak, M.; Sautier, B.; Spain, M.; Procter, D.J. Electron transfer reduction of nitriles using SmI<sub>2</sub>-Et<sub>3</sub>N-H<sub>2</sub>O: Synthetic utility and mechanism. *Org. Lett.* **2014**, *16*, 1092–1095. [[CrossRef](#)] [[PubMed](#)]
67. Lopez-De Jesus, Y.M.; Johnson, C.E.; Monnier, J.R.; Williams, C.T. Selective Hydrogenation of Benzonitrile by Alumina-Supported Ir-Pd Catalysts. *Top. Catal.* **2010**, *53*, 1132–1137. [[CrossRef](#)]
68. Molnar, A.; Smith, G.V.; Bartok, M. New catalytic materials from amorphous metal-alloys. *Adv. Catal.* **1989**, *36*, 329–383.
69. Li, H.; Xu, Y.; Li, H.; Deng, J.F. Gas-phase hydrogenation of adiponitrile with high selectivity to primary amine over supported Ni-B amorphous catalysts. *Appl. Catal. A-Gen.* **2001**, *216*, 51–58. [[CrossRef](#)]
70. Wang, W.-J.; Qiao, M.-H.; Li, H.-X.; Deng, J.-F. Partial Hydrogenation of Cyclopentadiene over Amorphous NiB Alloy on  $\alpha$ -Alumina and Titania-Modified  $\alpha$ -Alumina. *J. Chem. Technol. Biotechnol.* **1998**, *72*, 280–284. [[CrossRef](#)]
71. Chiang, S.-J.; Yang, C.-H.; Chen, Y.-Z.; Liaw, B.-J. High-active nickel catalyst of NiB/SiO<sub>2</sub> for citral hydrogenation at low temperature. *Appl. Catal. A-Gen.* **2007**, *326*, 180–188. [[CrossRef](#)]
72. Li, Y.; Zhu, G.; Wang, Y.; Chai, Y.; Liu, C. Preparation, mechanism and applications of oriented MFI zeolite membranes: A review. *Microporous Mesoporous Mater.* **2021**, *312*, 110790. [[CrossRef](#)]
73. Huybrechts, D.R.C.; Debruycker, L.; Jacobs, P.A. Oxyfunctionalization of alkanes with hydrogen-peroxide on titanium silicalite. *Nature* **1990**, *345*, 240–242. [[CrossRef](#)]

74. Lu, J.-Q.; Li, N.; Pan, X.-R.; Zhang, C.; Luo, M.-F. Direct propylene epoxidation with H<sub>2</sub> and O<sub>2</sub> over in modified Au/TS-1 catalysts. *Catal. Commun.* **2012**, *28*, 179–182. [[CrossRef](#)]
75. Nishimura, S. *Handbook of Heterogeneous Catalytic Hydrogenation for Organic Synthesis*; J. Wiley: New York, NY, USA, 2001.
76. Liu, Y.; Zhou, K.; Lu, M.; Wang, L.; Wei, Z.; Li, X. Acidic/Basic Oxides-Supported Cobalt Catalysts for One-Pot Synthesis of Isophorone Diamine from Hydroamination of Isophorone Nitrile. *Ind. Eng. Chem. Res.* **2015**, *54*, 9124–9132. [[CrossRef](#)]
77. Chojecki, A.; Veprek-Heijman, M.; Müller, T.E.; Schäringer, P.; Veprek, S.; Lercher, J.A. Tailoring Raney-catalysts for the selective hydrogenation of butyronitrile to n-butylamine. *J. Catal.* **2007**, *245*, 237–248. [[CrossRef](#)]
78. Gluhoi, A.C.; Mărginean, P.; Stănescu, U. Effect of supports on the activity of nickel catalysts in acetonitrile hydrogenation. *Appl. Catal. A-Gen.* **2005**, *294*, 208–214. [[CrossRef](#)]
79. Huang, J.; Han, J.; Wang, R.; Zhang, Y.; Wang, X.; Zhang, X.; Zhang, Z.; Zhang, Y.; Song, B.; Jin, S. Improving Electrocatalysts for Oxygen Evolution Using Ni<sub>x</sub>Fe<sub>3-x</sub>O<sub>4</sub>/Ni Hybrid Nanostructures Formed by Solvothermal Synthesis. *ACS Energy Lett.* **2018**, *3*, 1698–1707. [[CrossRef](#)]
80. Li, H.; Li, H.X.; Dai, W.L.; Wang, W.J.; Fang, Z.G.; Deng, J.F. XPS studies on surface electronic characteristics of Ni-B and Ni-P amorphous alloy and its correlation to their catalytic properties. *Appl. Surf. Sci.* **1999**, *152*, 25–34. [[CrossRef](#)]
81. Jiang, W.J.; Niu, S.; Tang, T.; Zhang, Q.H.; Liu, X.Z.; Zhang, Y.; Chen, Y.Y.; Li, J.H.; Gu, L.; Wan, L.J.; et al. Crystallinity-Modulated Electrocatalytic Activity of a Nickel(II) Borate Thin Layer on Ni<sub>3</sub>B for Efficient Water Oxidation. *Angew. Chem. Int. Ed.* **2017**, *56*, 6572–6577. [[CrossRef](#)] [[PubMed](#)]
82. Wang, L.; Li, W.; Zhang, M.; Tao, K. The interactions between the NiB amorphous alloy and TiO<sub>2</sub> support in the NiB/TiO<sub>2</sub> amorphous catalysts. *Appl. Catal. A-Gen.* **2004**, *259*, 185–190. [[CrossRef](#)]